Dynamic Endoscopic Gaussian Reconstruction for Vascular Information Enhancement

Ling Li[1,2], Wenyuan Huang[2,3,4], Jia Gu[4] and Wenjian Qin[3,*]

[1] Guangdong Mechanical and Electrical Polytechnic, 510515 Guangzhou, China
[2] School of Physics and Optoelectronics, Xiangtan University, 411105 Xiangtan, China
[3] Shenzhen Institutes of Advanced Technology, Chinese Academy of Sciences, 518055 Shenzhen, China
[4] Faculty of Data Science, City University of Macau, 999078 Macau, China
* wj.qin@siat.ac.cn

Abstract. Reconstructing deformable tissues from endoscopic videos is a critical task in fields such as robot-assisted minimally invasive surgery, virtual reality, and augmented reality. Compared with neural radiance fields, the introduction of the 3D Gaussian Splatting technique (3DGS) significantly reduces the time required for 3D reconstruction and rendering while maintaining good image quality to a certain extent, offering new possibilities for real-time 3D rendering during endoscopic procedures. However, this technique suffers from a significant loss of image details during rendering, manifesting in endoscopic scenes as missing vascular details, which directly affects the accuracy of lesion localization by clinicians. To address this issue, this paper proposes a novel method for enhancing vascular information in dynamic endoscopic scene reconstruction. The proposed approach begins with image preprocessing, employing a lightweight and efficient vascular enhancement algorithm. By optimizing brightness, details, and contrast in the HSV color space, it enhances the visibility of vascular structures. Combined with the state-of-the-art 3DGS method for endoscopy, it improves the display of vascular details in 3D images. Experimental results demonstrate that, compared with the original 3D rendering and other 2D enhancement algorithms, the proposed method significantly enhances the visualization quality of vascular structures, effectively compensating for the shortcomings of the 3D Gaussian Splatting technique in vascular detail representation.

Keywords: Endoscopic Image; Vascular Enhancement; 3D Gaussian Splatting.

1 Introduction

Reconstruction of dynamic 3D scenes from endoscopic videos is crucial for robot-assisted minimally invasive surgery [1]. By visualizing 3D models of tissues, surgeons are able to simulate realistic surgical scenarios in virtual reality (VR) or augmented reality (AR) environments [2], enabling preoperative planning and surgical training. In addition, reconstruction techniques supporting real-time rendering can be directly applied to intraoperative scenarios, enabling surgeons to have a comprehensive view of the surgical scene, thus enabling precise navigation and control of surgical instruments and laying the foundation for automation of robotic surgery.

In the field of scene reconstruction, 3DGS has recently revolutionized radiation field reconstruction, enabling high-quality synthesis of new views and fast rendering speeds [3]. 3DGS [4] achieves real-time rendering and superior reconstruction quality by representing the scene as an anisotropic 3D Gaussian distribution and rendering it with an efficient tiling-based rasterizer. EndoGS [5], EndoGaussian [6] and Deform3DGS [7] have applied 3DGS to the task of reconstructing and rendering endoscopic scenes and demonstrated good rendering speed and quality.

However, as shown in Fig.1, the 3DGS method suffers from a lack of detail information during the reconstruction of the rendered model, and this lack manifests itself in the endoscopic images as an omission of key anatomical details such as blood vessels. These vascular details are not only extremely important for the surgeon to identify anatomical structures during the surgical planning stage, but also play a key role in intraoperative navigation, and thus enhancement of the vessels is required.

In this paper, from the perspective of Gaussian ellipsoid rendering optimization, a 3D reconstruction method for endoscopic videos with effectively enhanced vascular information is proposed. By designing a lightweight multi-scale fast guided filtering algorithm, the brightness, details and contrast of the image are optimized in the HSV color space to strengthen the prominence of the blood vessel information in the image, and then the enhanced image is used as the input of the endoscopic 3DGS method to optimize the Gaussian ellipsoid color, transparency, and other parameters, to achieve the effect of highlighting the blood vessels in the three-dimensional model. To evaluate the effectiveness of the method and algorithm, experiments were conducted on SCARED[8] and ENDONERF[9] data, respectively.

2 Related Work

2.1 3D Reconstruction Rendering Methods

In the field of surgical scene reconstruction, early SLAM-based methods [10] performed reconstruction by estimating depth from stereoscopic videos and fusing depth maps in 3D space, but ignoring the influence of surgical tools and assuming a static scene led to their limited effectiveness in reconstructing real surgical scenes. Subsequent improved methods, such as E-DSSR [11], introduced a tool-masked depth estimation framework to better handle the interference of surgical tools. However, these methods mainly rely on sparse distortion fields for deformation tracking, and there are still obvious limitations for processing complex dynamic scenes.

In recent years, the implicit reconstruction method of Neural Radiance Fields (NeRF) model has performed well in 3D reconstruction, and EndoNeRF [9] and EndoSurf [1] further applied it to medical scene reconstruction for high-fidelity 3D reconstruction of endoscopic images, but the training time was more than 10 hours. The emergence of new methods based on 3DGS has greatly reduced the rendering time, compressing the training time to less than 1 hour. Methods such as EndoGS [5], EndoGaussian [6] and Deform3DGS [7] outperform NeRF in terms of rendering speed

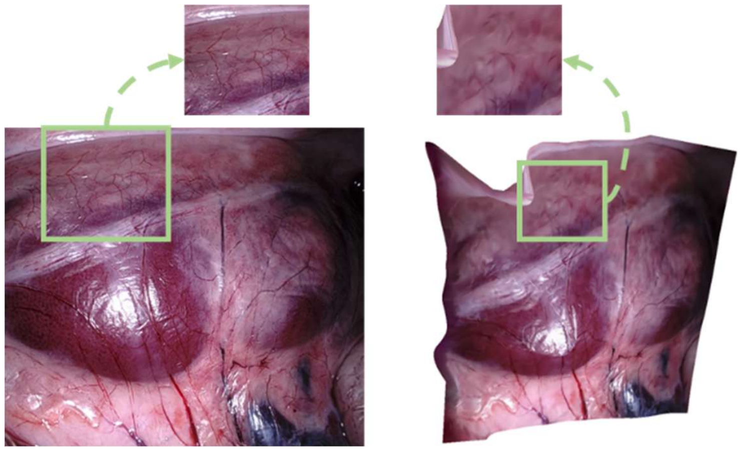

Fig. 1. Rendering of the EndoGaussian method

and quality, especially Deform3DGS which can complete the scene training in only 1 minute. However, existing endoscopic 3DGS methods suffer from problems such as missing vessel details after 3D reconstruction rendering, and need to be further optimized to meet the complex reconstruction needs of surgical scenes.

2.2 Vascular Enhancement Methods

In the field of vascular enhancement of medical images, existing algorithmic research has focused on retinal images and endoscopic images. Unlike the segmentation and enhancement of static vascular structures in retinal images, endoscopic videos have real-time and dynamic characteristics. In addition, the vascular enhancement process faces greater challenges due to the complexity of the internal human environment, including the diversity of tissue properties, changing lighting conditions, and the interference of motion artefacts, which puts higher demands on the research of more targeted and adaptive algorithms.

Existing research on endoscopic vascular enhancement has focused on the 2D processing of endoscopic video frames, using both learning-based and conventional approaches. A key challenge for learning-based methods is the acquisition of high-quality labels, and although the emergence of generative methods (e.g., GAN [12] and Diffusion [13]) offers new possibilities to address this issue, their application scope is still limited by the lack of clear and publicly available endoscopic image datasets. In addition, traditional methods dominate current research because they are more suitable for the needs of real-time endoscopic processing. For example, filter-based methods [14] highlight vessel details using enhancement techniques with different frequencies and orientations; and Retinex-based methods [15] significantly improve the overall quality of the image by ameliorating illumination irregularities and enhancing detail performance. However, existing vascular enhancement algorithms generally suffer from the lack of a fixed evaluation dataset, with most studies typically selecting only 5-6 public or private images for processing and evaluating the relevant metrics based on them, leaving their generalization capabilities unproven.

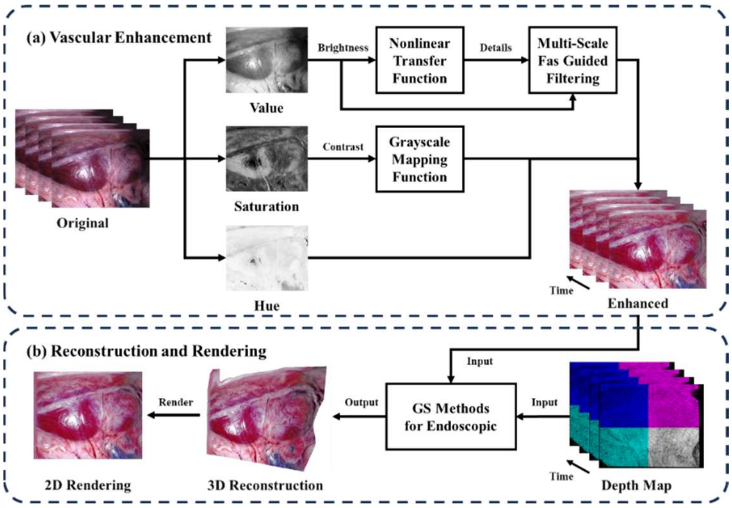

Fig. 2. A framework of dynamic endoscopic scene reconstruction methods for enhancing vascular information

3 Method

In this context, a dynamic endoscopic scene reconstruction method that can effectively enhance vascular information is proposed, as shown in Fig.2. The method preprocesses endoscopic images by combining vascular enhancement algorithms and completes the 3D reconstruction of tissues using 3DGS technology, thus achieving the enhancement and visualization of vascular information.

3.1 Vascular Enhancement Module

Compared to the RGB color space, the HSV color space is able to represent the hue, saturation and lightness of colors more intuitively, which is more conducive to enhancement of blood vessel details in an image. Therefore, the original image is first converted from the RGB domain to the HSV domain and the values of the H, S and V channels are extracted.

Enhancement of The Brightness Channel. In order to globally increase the image brightness and avoid the occlusion of blood vessel details by lower brightness and darker areas, the dynamic range compression technique was used to achieve adaptive adjustment of image brightness. In detail, the following nonlinear transfer function is used to process the brightness channel of the endoscopic image:

$$Vn = \frac{V^{0.75z+\ .25}+0.4(1-V)(1-z)+V^{(2-z)}}{2} \tag{1}$$

where Vn denotes the luminance channel of the processed image, V denotes the luminance channel of the original endoscopic image, and z denotes an adaptive adjustment factor. The parameter z is determined by the histogram of the image luminance channel, calculated in accordance with the following relationship:

$$z = \begin{cases} 0, \ L \leq 50 \\ \frac{L-50}{100}, \ 50 < L < 150 \\ 1, \ L \geq 150 \end{cases} \tag{2}$$

Wherein L is a grey level pixel intensity value calculated according to the cumulative distribution function of the image, specifically the pixel intensity corresponding to when the cumulative distribution function reaches 0.1.

Although overall brightness enhancement helps to improve the visibility of information in dark areas, the process is often accompanied by the introduction of additional noise, so further image denoising is particularly necessary. Compared with traditional gaussian and bilateral filtering methods, Fast Guided Filter (FGF) not only effectively removes noise, but also better preserves the image edge information, and at the same time has lower computational complexity, so it is more suitable for vascular enhancement and real-time processing of single-frame images of endoscopic videos.

In addition, the luminance channel not only reflects the overall lighting information, but also contains rich edge features which are often closely related to the vascular structure. By applying FGF, not only the new noise introduced by the brightness enhancement in dark areas can be reduced, but also the key edge details can be better preserved. The specific operation is the solution:

Firstly, it is assumed that the bootstrap image I and the filtered output image Q satisfy a linear model relationship in the local area, i.e:

$$Q_i = a_k I_i + b_k, \forall i \in \omega_k \tag{3}$$

where i is the pixel index and k denotes the pixel index of the local square window ω_k centred at pixel k with radius r; Q_i is the i-th pixel value in the filtered output image and I_i is the ith pixel value in the bootstrap image; and a_k and b_k are the linear filtering parameters within the corresponding window ω_k.

Given the filtered input image V, the local linear model parameters can be solved to obtain the local linear model parameters by minimizing the reconstruction error between V and Q:

$$a_k = \frac{\frac{1}{|\omega|}\sum_{i \in \omega_k} I_i V_i - \mu_k \bar{V}_k}{\sigma_k^2 + \epsilon} \tag{4}$$

$$b_k = \bar{V}_k - a_k \mu_k \tag{5}$$

where V_i denotes the i-th pixel in the filtered input image V and ϵ is a regularisation parameter controlling the smoothness; furthermore, $\bar{V}_k$ is the mean value of V within the window ω_k, and μ_k and σ_k are the mean and the standard deviation of the bootstrap image I in the window ω_k, respectively.

After calculating the filter parameters a_k and b_k within all windows ω_k in the image, the filter output Q_i can be determined by the following equation:

$$Q_i = \bar{a}_i I_i + \bar{b}_i \tag{6}$$

where $\bar{a}_i$ and $\bar{b}_i$ are the average values of a and b over a window ω_i centred on pixel i, respectively.

In order to further reduce the computational complexity, fast guided filtering significantly reduces the computation time while maintaining the spatial consistency and accuracy of the processing results by down sampling the filtered input image V and the guided image I, and then restoring them to the original resolution by up sampling after the filtering parameters a_k and b_k have been computed.

In fast oriented filtering, the size of the window ω directly affects the filtering effect: a smaller window captures the brightness information within the local neighborhood, while a larger window close to the image size reflects the global brightness change characteristics. Considering the differences in image denoising ability of different windows, we adopt a multi-scale filter design. Specifically, for each scale of filter output, we compare it with the pixel intensity of the original luminance image: if the intensity of the center pixel is higher than the average intensity of its surrounding pixels, the value of the pixel in the filter output image is increased accordingly; conversely, the value of the pixel is decreased. The exact formula for this process is as follows:

$$E_j(x, y) = \left\lfloor \frac{Q_j(x,y)}{V(x,y)} \right\rfloor^P \tag{7}$$

$$v_j(x, y) = V_n(x, y)^{E_j(x,y)} \tag{8}$$

where j denotes the j-th filtering; $E_j(x, y)$, $Q_j(x, y)$, and $V(x, y)$ denote the corresponding pixel values in the jth output, filtered output image, and filtered input image, respectively; $V_n(x, y)$ denotes the luminance channel of the processed endoscopic image, and P is an adaptive adjustment parameter, whose value is correlated with the global standard deviation σ of the filtered output image, and whose relationship is defined as follows:

$$P = \begin{cases} \frac{7}{4}, & \sigma \leq 2 \\ \frac{27-2\sigma}{13}, & 2 < \sigma < 10 \\ \frac{1}{2}, & \sigma \geq 10 \end{cases} \tag{9}$$

When $E_j(x, y) < 1$, it indicates that the centre pixel is brighter compared to the surrounding pixels; conversely, it indicates that the centre pixel is darker than the surrounding pixels. By this strategy, the change or degradation of image detail information due to brightness enhancement can be effectively avoided. Finally, the filtering results of each scale are averaged to obtain the final filtered image $V^*(x, y)$.

$$V^*(x, y) = \frac{\sum_j v_j(x,y)}{j} \tag{10}$$

This multi-scale fast oriented filtering method can better maintain the image edge details while effectively denoising, which meets the requirements of real-time and accuracy in endoscopic image vascular enhancement processing. For this reason, in our experiments, we used three different sizes of windows (4, 16, and 64) to filter the input image multiple times to achieve the vascular enhancement effect of the luminance channel.

Enhancement of The Saturation Channel. While the luminance channel is processed, the saturation channel, as a key factor reflecting the color vibrancy of the image, also receives attention in this study. Through the enhancement algorithm, the overall vividness of the image can be enhanced, and the color saturation of the region around the blood vessels can be specifically enhanced, thus making the blood vessels more prominent in the image and helping to accurately display the location and morphology of the blood vessels. Specifically, the contrast stretching method is applied to the S component, and its mapping function is defined as:

$$S^* = [1 + d \times (S^{-1} - 1)^2]^{-1} \tag{11}$$

Where: S and S^* are the S-channel grey values before and after mapping, respectively; d is the S-channel grey mapping parameter, which is calculated as:

$$d = \frac{3S_m^2 - 2S_m^3}{2S_m^3 - 3S_m^2 + 1} \tag{12}$$

where S_m is the grey mean value of the saturation channel before mapping. This mapping function achieves the saturation contrast stretching of the region of interest in the image by adjusting the distribution characteristics of the S component to enhance the blood vessel visualisation.

3.2 Reconstruction and Rendering Module

3DGS [6] is an explicit 3D scene representation in the form of a point cloud. It is a static 3D scene representation that models the scene as a 3D Gaussian point cloud in the world coordinate system. In the reconstruction part, the 3D point cloud is estimated and initialized by the SfM method from a set of images to obtain a set of 3D Gaussian distributions. In the rendering part, each 3D Gaussian matrix is characterized by a covariance matrix Σ and a centroid X, which is called the mean of the Gaussian matrix:

$$G(X) = \exp\left(-\frac{1}{2}X^{\mathrm{T}}\Sigma^{-1}X\right) \tag{13}$$

For a differentiable optimization, the covariance matrix Σ can be decomposed into a scaling matrix S and a rotation matrix R. The covariance matrix Σ can be decomposed into a rotation matrix R and a scaling matrix S:

$$\Sigma = RSS^{\mathrm{T}}R^{\mathrm{T}} \tag{14}$$

When rendering a new view, the difference splat [17] is used for a 3D Gaussian distribution in the camera plane. By using the Jacobi matrix J of the affine approximation of the observation transformation matrix W and the projective transformation, the covariance matrix Σ' in the camera coordinates can be computed as:

$$\Sigma' = JW\Sigma W^{\mathrm{T}}J^{\mathrm{T}} \tag{15}$$

Each Gaussian point contains learnable attributes: position $X \in \mathbb{R}^3$, color defined by the spherical harmonic (SH) coefficient $C \in \mathbb{R}^k$ (k is the number of SH functions), opacity α , rotation angle $r \in \mathbb{R}^4$, and scale $s \in \mathbb{R}^3$. Specifically, for each pixel, the colours and opacities of all the Gaussian distributions are computed using equation (13). The blending of the N ordered points overlapping the pixel is given by the following equation:

$$C = \sum_{i \in N} c_i \alpha_i \prod_{j=1}^{i-1} (1 - \alpha_i) \tag{16}$$

where c_i, α_i denote the density and colour of the point, which is calculated by multiplying the 3D Gaussian G with covariance Σ by the optimisable per-point opacity and SH colour coefficients.

There have been studies applying 3DGS methods to endoscopic 3D rendering tasks and incorporating their respective optimization strategies to enhance the reconstruction results. However, compared with the EndoGS method, the EndoGaussian and Deform3DGS methods show better results in the reconstruction rendering of 3D scenes. Therefore, in this study, the above two methods are selected as a combination object to experimentally verify the performance difference of the proposed methods and their effectiveness in enhancing the vascular information in the 3D reconstruction task of dynamic endoscopic videos.

4 Results

Desktop with Intel® Xeon® E5-2650 v4 CPU, NVIDIA Tesla P100 16GB GPU and Ubuntu 22.04.4 LTS. Laptops with Intel® Core™ i5-12500H CPU, 16GB RAM (4800MHz) and Windows 11.

4.1 Evaluation of Rendering Results

Compared to the RGB color space, the HSV color space is able to represent the hue, saturation and lightness of colors more intuitively, which is more conducive to enhancement of blood vessel details in an image. Therefore, the original image is first converted from the RGB domain to the HSV domain and the values of the H, S and V channels are extracted.

We use the vascular enhancement algorithm for the preprocessing of two open-source datasets, SCARED and ENDONERF, where the regularization and scaling parameters of the fast guided filtering are chosen as $\epsilon = 0.05^2$, and s = 2, respectively, and the parameter of grey-scale mapping function is chosen as 0.5 d_s. By using the original and the algorithmically enhanced maps as the input images, we use the EnDoGaussian and Deform3DGS methods for 3000 continuous iterations according to their respective initial parameters (where the initial learning rate is uniformly 1.6×10^{-3}), and compared the output reconstructed rendered images (the reconstructed 3D model takes the 2D image rendered by a single camera view) in terms of the detail variance (DV), the background variance (BV), and the detail variance/background variance (DV/BV) values, and the experimental results are shown in Tables 1 and 2.

Table 1. Combine the performance of the EndoGaussian method on the SCARED and ENDONERF datasets comparison.

Datasets	Input	LPIPS↓	DV↑	BV↓	DV/BV↑
Scared	Original	0.2754	**1146.07**	547.67	2.11
Dataset_1	Ours	**0.2625**	968.94	**432.26**	**2.41**
Scared	Original	0.2124	944.91	766.86	1.26
Dataset_2	Ours	**0.2121**	**1131.84**	**657.86**	**1.72**
Scared	Original	**0.4348**	895.15	589.66	1.55
Dataset_3	Ours	0.4399	**1054.38**	**490.86**	**2.16**
Scared	Original	**0.4529**	**742.05**	494.52	1.50
Dataset_6	Ours	0.4779	689.06	**395.32**	**1.78**
ENDONERF	Original	**0.102**	521.72	487.87	1.07
cutting	Ours	0.115	**741.30**	**460.64**	**1.61**
ENDONERF	Original	**0.106**	259.68	**218.77**	1.21
pulling	Ours	0.122	**427.55**	243.74	**1.76**

Table 2. Combined with the Deform3DGS method, the performance on the ENDONERF dataset compares.

Datasets	Input	LPIPS↓	DV↑	BV↓	DV/BV↑
ENDONERF	Original	**0.064**	414.71	779.48	0.54
cutting	Ours	0.068	**572.00**	**560.22**	**1.02**
ENDONERF	Original	**0.042**	651.04	706.03	0.93
pulling	Ours	0.043	**871.14**	**596.63**	**1.47**

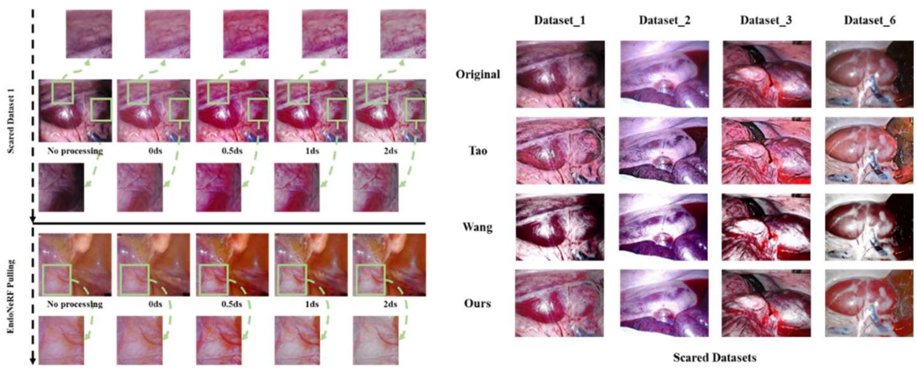

Fig. 3. Comparison of rendering results (Left); Comparison of enhancement results (Right).

The results show that our method has a significant improvement in the core DV/BV metric, which is commonly used to measure the contrast between blood vessels and the background in endoscopic images. A higher DV/BV ratio indicates that blood vessels are more clearly distinguished from the background in the image [18].

In order to provide an intuitive comparison of the visual effects, we show the rendering results of two different datasets combined with the EndoGaussian method in Fig. 3 (Left). It can be observed that when processing in the luminance channel only (0ds), our method is able to reveal otherwise undisplayable blood vessel information in the dark areas of the image, and the noise in the dark areas can be smoothed to some extent. And after adding the saturation channel processing (0.5ds/1ds/2ds), the blood vessels in the edge region of the image are better preserved and displayed. In addition, after dataset enhancement, the blood vessel details become more obvious in the whole image and are presented more intuitively.

4.2 Comparative Evaluation of Algorithms

In this section, we used MATLAB R2022a to conduct experiments on a laptop, comparing the original images, Tao [19], Wang [20] and our proposed algorithm (regularization and scaling parameters of fast guided filtering were chosen as $\epsilon = 0.05^2$, and s = 2, respectively, and the parameters of grey scale mapping function were chosen as d_s). Considering that the ENDONERF images contain surgical instruments, only SCARED was chosen for the experimental dataset.As can be seen in Table 3, our method performs the best in the core DV/BV metrics, indicating that the blood vessels in the processed images are able to be more clearly distinguished from the background.

Table 3. Performance comparison on the SCARED dataset.

Datasets	Input	DV↑	BV↓	DV/BV↑
Scared Dataset_1 (196 Pictures)	Original	1146.22	683.07	1.68
	Tao	786.95	1169.02	0.67
	Wang	**1756.08**	**1216.13**	1.44
	Ours	924.83	533.83	**1.73**
Scared Dataset_2 (87 Pictures)	Original	1037.03	**970.60**	1.08
	Tao	1138.25	1198.96	0.94
	Wang	**1436.33**	1476.24	0.98
	Ours	1304.15	1105.43	**1.19**
Scared Dataset_3 (328 Pictures)	Original	1104.26	**667.84**	1.67
	Tao	783.52	1264.58	0.62
	Wang	**1588.03**	1215.56	1.31
	Ours	1363.91	737.45	**1.87**
Scared Dataset_6 (636 Pictures)	Original	920.54	596.05	1.54
	Tao	689.95	778.27	0.89
	Wang	**1594.82**	1200.25	1.33
	Ours	893.30	**549.15**	**1.66**

To provide an intuitive visual effect, Fig. 3 (Right) demonstrates the effect of the four sub-datasets of SCARED. It can be observed that although Tao's method can effectively enhance the detailed features and improve the dark area information, the red blood vessels are mistakenly colored as black due to the processing of the G-channel, which significantly affects the doctor's judgement. On the other hand, although the method of Wang enhances the display of blood vessel details to a certain extent, the lack of brightness adjustment results in unidentified highlights in the central region of the image, which seriously interferes with the judgement of blood vessel features. As can be seen from the figure, our designed algorithm performs the best in terms of visual effect, which not only reveals the hidden information in the dark area, but also demonstrates the blood vessel features and tissue details more intuitively.

Combining visual effects and evaluation metrics, our proposed algorithm shows better results and higher robustness in the task of vascular enhancement of endoscopic images compared to other enhancement algorithms.

5 Conclusion

In summary, this study proposes a vascular information enhancement reconstruction method for dynamic endoscopic scenes. By designing a lightweight and efficient vascular enhancement algorithm to preprocess the input image of the 3DGS method, the detailed representation of blood vessels in the endoscopic 3D reconstruction model is effectively enhanced. From the assessment of quantitative indexes and visual effects, the reconstruction rendering after data preprocessing significantly compensates the deficiency of 3D Gaussian splatting methods in the representation of vascular details, and the accurate rendering of vascular details is of great significance for doctors' diagnosis and operation in the field of minimally invasive surgery. In addition, existing endoscopic 3DGS methods present explicit 3D scenes in the form of point clouds, and the reconstructed models lack editability due to their point-cloud representation [21]. In the future, if the reconstruction of dynamic mesh models [22] can be realized and combined with the enhancement of vascular information, it will provide richer and more flexible content for the surgical simulation scene, which will be one of the key directions for subsequent research.

References

1. Zha, R., Cheng, X., Li, H., et al.: EndoSurf: Neural Surface Reconstruction of Deformable Tissues with Stereo Endoscope Videos. In: Medical Image Computing and Computer Assisted Intervention – MICCAI 2023. MICCAI 2023. Lecture Notes in Computer Science, vol 14228. Springer, Cham (2023).
2. Schneider, M., Kunz, C., Pal'a, A., et al.: Augmented reality-assisted ventriculostomy. Neurosurgical focus 50(1), E16 (2021).
3. Huang, B., Yu, Z., Chen, A., et al.: 2D Gaussian Splatting for Geometrically Accurate Radiance Fields. In: ACM SIGGRAPH 2024 Conference Papers (SIGGRAPH '24), Article 32, pp. 1–11 (2024).
4. Kerbl, B., Kopanas, G., Leimkühler, T., et al.: 3D Gaussian Splatting for Real-Time Radiance Field Rendering. ACM Transactions on Graphics (TOG). 42(4): 1-14 (2023).

5. Zhu, L., Wang, Z., Cui, J., et al.: EndoGS: Deformable Endoscopic Tissues Reconstruction with Gaussian Splatting. In: Medical Image Computing and Computer Assisted Intervention – MICCAI 2024 Workshops. MICCAI 2024. Lecture Notes in Computer Science, vol 15274. Springer, Cham (2025).
6. Liu, Y., Li, C., Yang, C., et al.: EndoGaussian: Real-time Gaussian Splatting for Dynamic Endoscopic Scene Reconstruction. ArXiv (2024).
7. Yang, S., Li, Q., Shen, D., et al.: Deform3DGS: Flexible Deformation for Fast Surgical Scene Reconstruction with Gaussian Splatting. In: Linguraru, M.G., et al. Medical Image Computing and Computer Assisted Intervention – MICCAI 2024. MICCAI 2024. Lecture Notes in Computer Science, vol 15006. Springer, Cham (2024).
8. Allan, M., McLeod, J., Wang, C., et al.: Stereo Correspondence and Reconstruction of Endoscopic Data Challenge. ArXiv (2021).
9. Wang, Y., Long, Y., Fan, S.H., et al.: Neural Rendering for Stereo 3D Reconstruction of Deformable Tissues in Robotic Surgery. In: Medical Image Computing and Computer Assisted Intervention – MICCAI 2022. MICCAI 2022. Lecture Notes in Computer Science, vol 13437. Springer, Cham (2022).
10. Zhou, H., Jagadeesan, J.: Real-Time Dense Reconstruction of Tissue Surface From Stereo Optical Video. IEEE Transactions on Medical Imaging 39(2), 400–412 (2020).
11. Long, Y., Li, Z., Yee, C.H., et al.: E-DSSR: Efficient Dynamic Surgical Scene Reconstruction with Transformer-Based Stereoscopic Depth Perception. In: Medical Image Computing and Computer Assisted Intervention – MICCAI 2021. MICCAI 2021. Lecture Notes in Computer Science(), vol 12904. Springer, Cham (2021).
12. Daher, R., Vasconcelos, F., Stoyanov, D.: A Temporal Learning Approach to Inpainting Endoscopic Specularities and Its Effect on Image Correspondence. Medical Image Analysis 90, 102994 (2023).
13. Kaleta, J., Dall'Alba, D., Płotka, S., et al.: Minimal data requirement for realistic endoscopic image generation with Stable Diffusion. International Journal of Computer Assisted Radiology and Surgery 19(3), 531–539 (2024).
14. Zhang, G., Lin, J., Cao, E., et al.: A Medical Endoscope Image Enhancement Method Based on Improved Weighted Guided Filtering. Mathematics 10(9), 1423 (2022).
15. Luo, X., Zeng, H.Q., Wan, Y., et al.: Endoscopic Vision Augmentation Using Multiscale Bilateral-Weighted Retinex for Robotic Surgery. IEEE Transactions on Medical Imaging 38(12), 2863–2874 (2019).
16. Zhao Y, Zhang J, Pereira E, et al.: Automated tortuosity analysis of nerve fibers in corneal confocal microscopy. IEEE transactions on medical imaging 39(9), 2725–2737 (2020).
17. Yifan W, Serena F, Wu S, et al.: Differentiable Surface Splatting for Point-based Geometry Processing. ACM Transactions On Graphics (TOG). 38(6): 1-14 (2019).
18. Hongpeng J, Kejian Z, Bo Y, et al.: A vascular enhancement algorithm for endoscope image. Opto-Electronic Engineering, 46(1): 180167-1-180167-9 (2019).
19. Tao L, Asari V K: Adaptive and integrated neighborhood-dependent approach for non-linear enhancement of color images. Journal of Electronic Imaging, 14(4): 043006. (2005).
20. Qiang W, Pei T, Bo Y, et al.: Vessel enhancement of endoscopic image based on multi-color space. Opto-Electronic Engineering, 47(1): 190268-1-190268-6 (2020).
21. Huang W, Zhang Q, Gu J, et al.: High-Quality Gaussian Surface Mesh Reconstruction for Endoscopic Deformable Tissue. In: 2025 8th International Symposium on Big Data and Applied Statistics (ISBDAS). IEEE, 645-648 (2025).
22. Jiang Y, Yu C, Xie T, et al.: VR-GS: A Physical Dynamics-Aware Interactive Gaussian Splatting System in Virtual Reality. In ACM SIGGRAPH 2024 Conference Papers (SIGGRAPH '24). Article 78, 1 (2024).